

INVESTIGATION OF CHEVRON CATHODE PADS FOR POSITION ENCODING IN VERY HIGH RATE, GAS PROPORTIONAL CHAMBERS*

B. Yu, G. C. Smith, V. Radeka

Brookhaven National Laboratory, Upton, NY 11973

and

E. Mathieson

Leicester University, Leicester LE1 7RH, England

Abstract

New techniques for position encoding in very high rate particle and photon detectors will be required in experiments planned for future particle accelerators such as the Superconducting Super Collider and new, high intensity, synchrotron sources. We are carrying out a detailed theoretical and experimental study of a position interpolation technique in which a row of chevron shaped cathode pads lies underneath each anode wire of a proportional chamber. Centroid finding of the cathode induced charge is performed on the signals from the chevron pads. High event rate and high multiplicity capabilities are achieved by parallel readout. Results are presented which illustrate the reduction, to an acceptably low level, of differential non-linearity by specific changes in the chevron geometry, position resolution of about $110\ \mu\text{m}$ (FWHM) for 5.4 keV X-rays independent of wire length, and the role played by avalanche angular localization in the position interpolation technique.

I. INTRODUCTION

An important requirement that is common to position sensitive detector development in many fields, is an increase in counting rate capability. In high energy physics, for example, experiments at heavy ion colliders and hadron colliders (such as the Superconducting Super Collider) will require accurate tracking detectors capable of resolving very high multiplicity events. In synchrotron radiation experiments, the next generation of synchrotron sources will increase the maximum photon flux beyond the capabilities of many present position encoding methods.

Most global position encoding techniques limit the detector to analyzing one event at a time. With silicon detectors, the so-called pixel detector achieves a very large increase in counting rate capability through the use of many parallel readout channels. With wire proportional chambers interpolating cathode pads for high rate particle detectors [1,2] have recently been investigated. These are not actual pixel devices but, nevertheless, they achieve the desired goal of increased counting rate by subdivision of the cathode position encoder into many independent readout channels.

In this paper we report on an extended study of interpolating cathode pads which were the subject of preliminary tests described in Ref. [1]. In this technique there is a row of cathode pads underneath each anode wire, so that the complete cathode is one large array of pads. Each row of pads has its own electronic readout, with position resolution along an anode wire being determined by the nature of this readout and the pad geometry. Position resolution in the other direction is generally limited to the anode wire spacing. Essentially each anode wire has its own position encoder, and maximum detector event rate is therefore significantly increased. The cathode induced charge has a bell-shaped distribution with a full width at half maximum of approximately 1.5 times the anode, cathode spacing; the cathode pads sample this distribution, the centroid of which allows the position of an event along the anode wire axis to be determined. Using a specific chamber configuration, the present work examines the behavior of position non-linearity with pad geometry, cathode signal shaping time, and anode avalanche angular localization.

II. CHEVRON PADS

An early use of electrodes with a specific geometric shape to perform centroid determination of a spatially extended signal was developed by Anger [3]. Subsequently, there have been several position encoding schemes based on geometric charge division, for example Refs. [4-7]. Chevron pads work on the same general principle, using a specific geometric shape to sample, and find the centroid of, cathode induced charge. This allows a substantially larger readout node spacing to be used than if standard rectangular pads were used. Chevron pads are a special form of the zigzag cathode [8,9], which was developed to reduce the number of readout channels in global position encoding with multiwire chambers.

Three types of chevron, each with two versions, have been investigated in this work; the six chevron patterns are shown in Figs. 1(a)-(f). The first type is the 'single chevron', which can be configured so that the anode wire runs over the chevron apex (Fig. 1(a)), or runs midway between the chevron apices (Fig. 1(b)). For convenience, these will be referred to as the centered single chevron

*This research was supported in part by the U.S. Department of Energy: Contract No. DE-AC02-76CH00016.

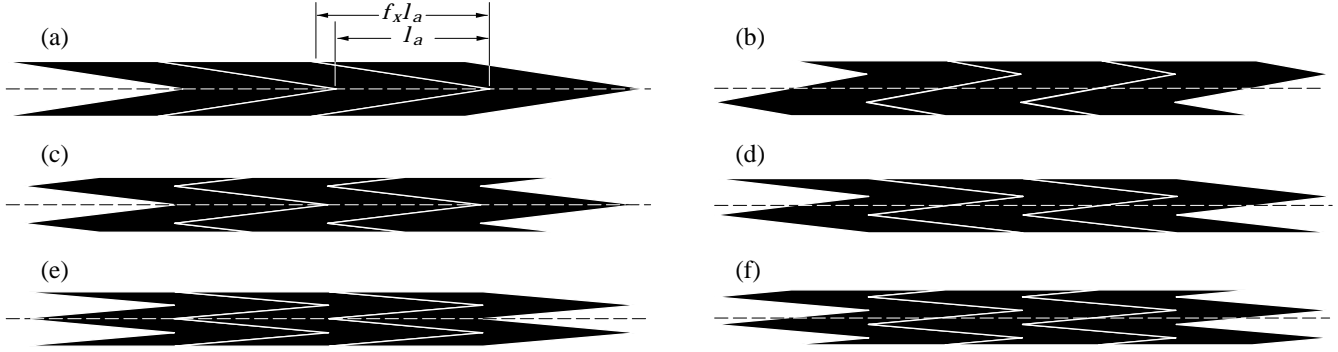


Figure 1: Patterns of (a) centered single chevron (b) displaced single chevron (c) centered one & a half chevron (d) displaced one & a half chevron (e) centered double chevron (f) displaced double chevron. Dashed line indicates anode wire position.

and displaced single chevron. In a similar way, we have constructed centered and displaced versions of ‘one & a half chevron’ pads (Fig. 1(c) and (d) respectively) and centered and displaced versions of ‘double chevron’ pads (Fig. 1(e) and (f) respectively).

We define the pad, or node, spacing to be l_a ; the depth of the chevron pattern is then defined to be $f_x l_a$, as shown in Fig. 1. In the work reported here we have used a fixed value of l_a and investigated the chevron performance as a function of f_x .

III. APPARATUS

A small test detector, which is shown schematically in Fig. 2, has been constructed specifically for this investigation. The anode, cathode spacing is 2mm, and anode wire spacing is 4mm, (diameter $18 \mu\text{m}$). There are field wires (diameter $125 \mu\text{m}$), also with spacing of 4mm, between anode wires. The cathode pad plane is fabricated from multi-layer printed circuit board (more details are given in Section V), while the window, or upper cathode, is $25 \mu\text{m}$ thick aluminized mylar. The row of chevron pads under an anode wire is 3.05 mm wide, with pads on centers given by $l_a = 12 \text{ mm}$.

Each row of cathode pads is separated from its neighboring row by a guard strip of width 0.95 mm, whose main purpose is to make insignificant the quantity of charge induced on the neighboring row. These basic chamber parameters are based on those of a much larger pad detector which is currently being used in a BNL heavy ion experiment [1].

Essentially, each anode wire sits at the center of a cell whose cross section is 4mm by 4mm, and whose boundaries are defined by the field wires. The test detector contains three active pad rows. Each of the cathode pads in a row is connected to one of two different sets of position encoding electronics:

- a) each pad in one row is connected to a charge sensitive preamplifier and shaping amplifier; a centroid is then

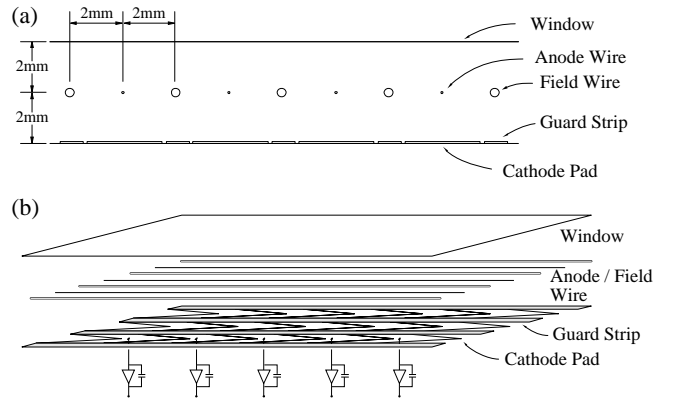


Figure 2: (a) Side view of detector (b) Exploded view (centered single chevrons used)

determined by analysis with a purpose built, centroid finding electronic system [10]. Most of the measurements were carried out with this configuration, which had signal shaping times of $1.4 \mu\text{sec}$ and 500 nsec .

- b) each pad in one row is connected to a delay line whose signal timing characteristics allow an accurate center of gravity of the anode avalanche to be determined [11]. This configuration allowed us to reduce the signal shaping time to 100 nsec .

The detector could be irradiated with 5.4 keV photons from an intense CrK X-ray source, either uniformly over the entire window or in collimated form with a $25 \mu\text{m}$ pencil beam.

IV. NON-LINEARITY

A. Non-linearity as a function of f_x

Nearly exact calculations of non-linearity can be carried out using a ‘single parameter’, empirical distribution of cathode charge [12]. It was found that a gaussian distribution, whose FWHM is adjusted to give a best

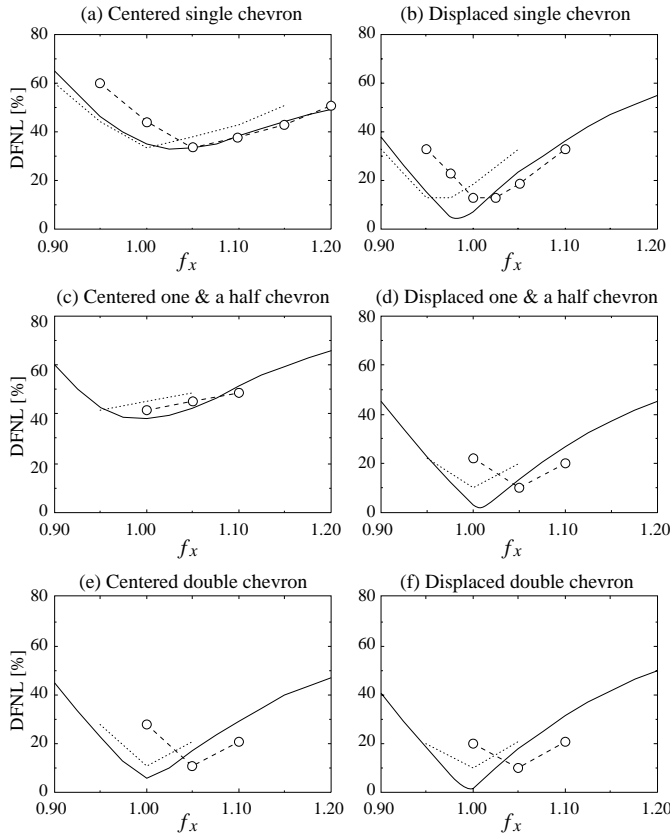


Figure 3: Differential non-linearity (DFNL) vs. f_x for (a) centered single chevron (b) displaced single chevron (c) centered one & a half chevron (d) displaced one & a half chevron (e) centered double chevron (f) displaced double chevron. See text for details.

fit to the calculations using the empirical distribution, yielded results which were very close to those from the correct distribution, and was somewhat easier to compute. Thus, all the theoretical predictions which follow have been calculated with the best fit gaussian induced charge distribution.

The continuous lines in Figs. 3(a)–(f) show the predicted behavior of differential non-linearity (DFNL), as a function of f_x , for the six chevron patterns illustrated in Fig. 1. (The numerical evaluation of DFNL is given in part B of this section.) There is a trend common to all six curves, namely that DFNL has a minimum at, or very close to, $f_x = 1.0$. Displaced versions of a particular chevron type always yield a better DFNL, at a given f_x , than the centered counterpart. This advantage is especially significant for the single, and one & a half, chevron types. The same effect was also observed with zigzag cathodes [9]. However, the effects of avalanche angular localization, which will be discussed in Section VI, can cause undesirable effects which are more significant for the displaced chevron than for the centered chevron, and the choice of a particular chevron pattern should not be based on DFNL alone. As one might expect, the performance of zigzag cathodes [9]

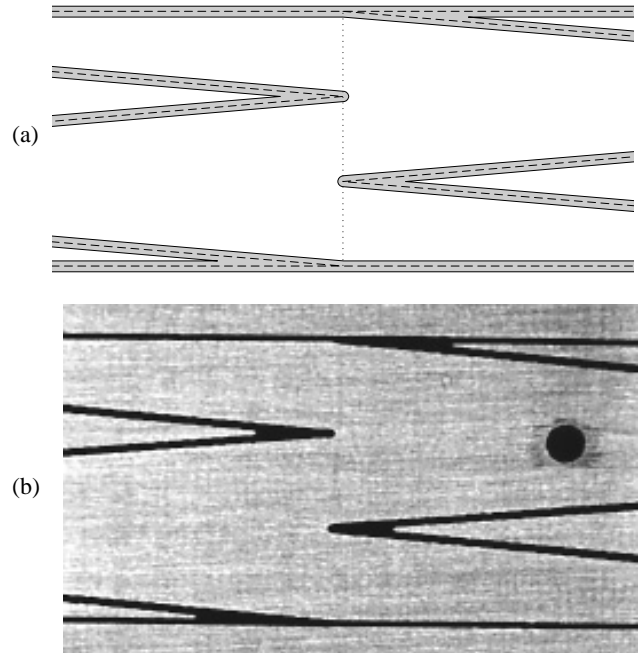


Figure 4: Enlarged view of chevron apices on displaced one & a half chevron, $f_x = 1.0$. (a) Design drawing, the gap width is exaggerated. (b) Photograph of same area of actual cathode (black circle is top of plated-through hole).

also showed that minimum DFNL was attained when the anode wires passed between the apices of the pattern.

Experimental measurements of DFNL have been performed by uniformly irradiating the test chamber with a broad beam of X-rays. The resulting uniform irradiation response (UIR) was obtained by analyzing signals from the position encoding electronics with a pulse height analyzer (PHA). Values of experimental DFNL are shown by the open circles in Fig. 3. There is, in general, quite good agreement between prediction and measurement, save for the fact that the curve through the measurements is displaced by about $f_x = +0.05$ in the abscissa, relative to prediction. We have attempted to illustrate this point by redrawing the experimental curve, in the form of a dotted line, with a displacement of $f_x = -0.05$. A similar phenomenon was also observed with zigzag cathodes [9].

Figure 4(a) shows a magnified area of part of the design artwork for the displaced one & a half chevron. The dashed lines represent the theoretical boundaries between adjacent pads, while the solid lines outline the area which, in practice, is etched away. As shown by the vertical dotted line, the chevron apices and bases should all be in line for this configuration with $f_x = 1.0$, but the etched gap pulls the apices away from each other. Figure 4(b) shows a photograph of the same area of the actual cathode; with our best print and etch techniques we can presently achieve, with uniformity and reliability, a gap of about $60\ \mu\text{m}$. For this particular cathode, the

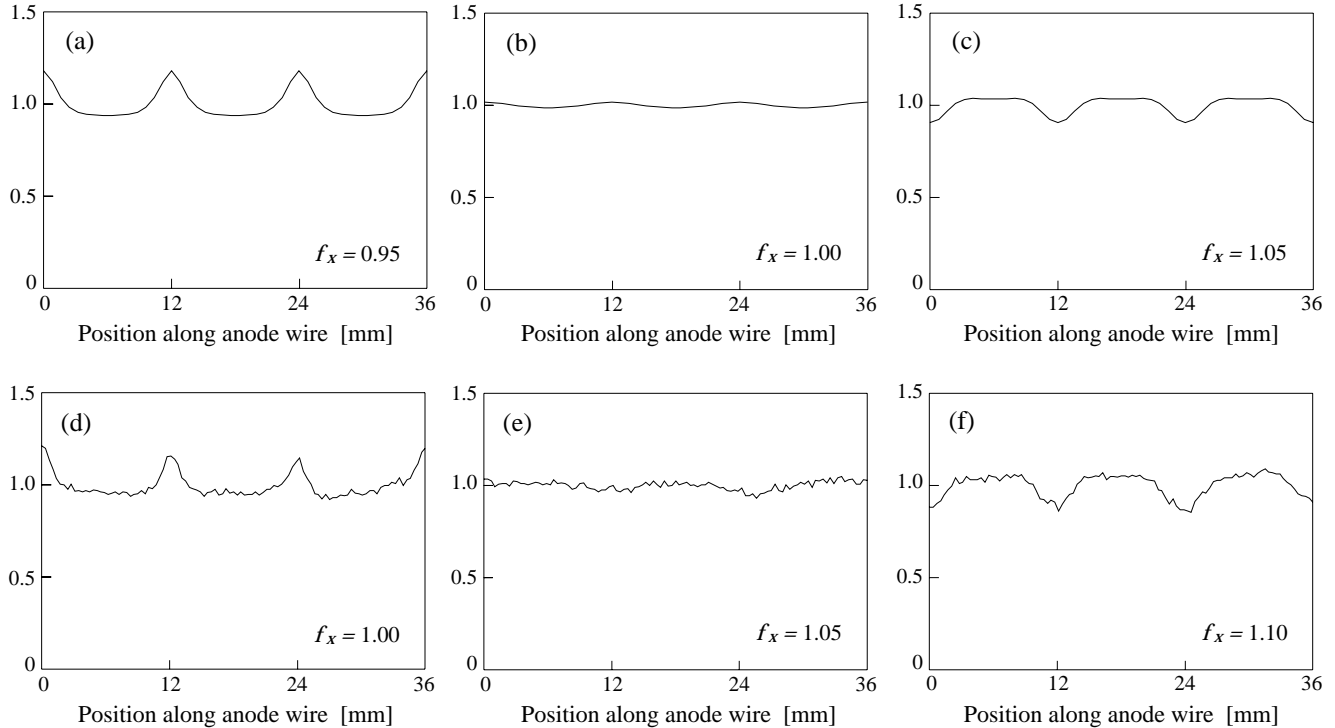


Figure 5: Uniform irradiation response (UIR) of displaced one & a half chevron pattern. (a)–(c) are theoretical predictions, (d)–(f) are experimental results.

apices of the chevrons are separated, in the axis of the anode wire, by about 1.5 mm, or 12% of the pad spacing l_a . Because the theoretical prediction takes no account of the gap between adjacent pads, we believe this is the main reason that the curve through the measured DFNL data is shifted to larger f_x relative to the theoretical prediction.

Not surprisingly, there is an overall increase in DFNL if the width of the gap between adjacent pads is allowed to increase. In some preliminary tests we performed on single chevrons, the DFNL more than doubled when the gap width was increased by two.

B. One & a half chevron UIR

DFNL is defined as

$$\text{DFNL} = \frac{(I_{\max} - I_{\min})}{(I_{\max} + I_{\min})/2},$$

where I_{\max} and I_{\min} are, respectively, the maximum and minimum points in the UIR. However, in comparing theory with experiment, the shape of the UIR is really as important as the value of DFNL. Using the one & a half displaced chevron as an example, Fig. 5 illustrates the predicted and experimental UIRs for the displaced one & a half chevron. Figure 5(a) shows predicted UIRs for $f_x = 0.95$, 1.0 and 1.05, while Fig. 5(b) shows experimental UIRs for $f_x = 1.0$, 1.05 and 1.1. The offset of 0.05 in these comparisons is intentional, in order to further

illustrate the effect described in part A of this section. It can be clearly seen that there is good agreement between the shape of the predicted and experimental spectra.

V. POSITION RESOLUTION

The chevron pads are fabricated on a three layer, 0.75 mm thick, printed circuit board; the pads themselves are on the front layer, and are connected via plated-through holes to conducting readout lines on the rear layer; the middle layer is a continuous ground plane 0.25 mm from the rear (broken, of course, at each of the plated holes) to minimize coupling between readout lines and the chevron pads. Each pad, therefore, has quite a large capacitance to ground, of order 20 pF. However, using the centroid finding electronics [10], with a spacing of only 12 mm between readout nodes, minimum position resolution is not limited by electronic noise.

Position resolution was measured by using a pencil beam of X-rays, energy 5.4 keV, and is shown as a function of anode charge in Fig. 6. All the chevron patterns exhibit similar position resolution characteristics. At low anode charge, less than about 0.08 pC, the resolution is electronic noise limited, but at higher charge levels it gradually reaches a plateau level of just over $110 \mu\text{m}$, which is consistent with the limit of resolution due to photoelectron and Auger electron range [13].

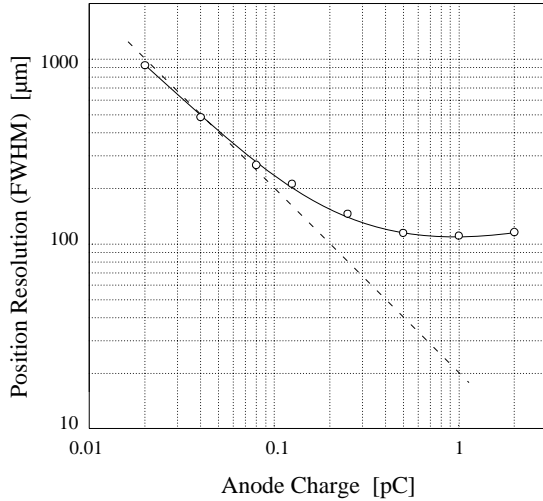


Figure 6: Position resolution vs anode charge, using centroid finding electronics

VI. EFFECTS DUE TO AVALANCHE ANGULAR LOCALIZATION

X-rays, unlike particle tracks, produce almost point-like deposits of primary ionization which, at low to moderate avalanche size, will create an anode avalanche which is localized to a small part of the anode wire circumference, depending upon which field lines the primary ionization has drifted. In very simple terms, we can distinguish between four types of events. The first are due to X-rays which have been absorbed between the anode wire and the cathode pad plane, and the second to those absorbed between the anode wire and the window; these are referred to as ‘pad side’ and ‘window side’ events, respectively. The third are due to X-rays absorbed between the anode wire and its neighboring left side field wire, say, and the fourth are due to X-rays absorbed between the anode and its neighboring right side field wire. As we shall see, these last two types of event can result in position errors due to ‘centroid shift’.

A. Pad side and Window side events

In any position encoding system which relies upon geometric charge division there will be, for a fixed cathode pattern, an increase in non-linearity of the encoded position as the ‘footprint’ of sampled charge becomes smaller. As a consequence, window side events are analyzed more linearly than pad side events, and this effect can cause a serious degradation in position resolution. There are certain characteristics of cathode signal shapes [14] that allow a determination to be made of which side of the anode plane an X-ray was absorbed; we have employed this electronic selection technique to measure, separately, the position linearity of pad side and window side events.

Figure 7 shows the absolute position error for the three chevron types used in this investigation, using the

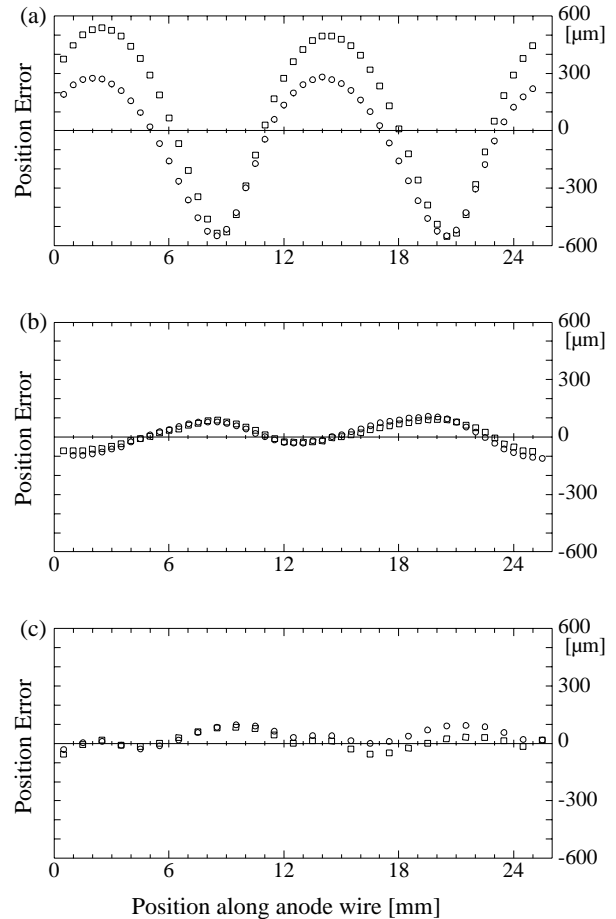


Figure 7: Position error of pad side (squares) and window side (circles) events vs. position along anode wire. (a) centered single chevron, $f_x = 1.05$ (b) displaced one & a half chevron, $f_x = 1.05$ (c) centered double chevron, $f_x = 1.05$

f_x values which gave minimum differential non-linearity (Section IV). For the single chevron there is a maximum position error of about $\pm 600 \mu\text{m}$ but, perhaps more seriously, there is a separation in position between pad and window side events which reaches a maximum of about $300 \mu\text{m}$. For both the one & a half and double chevron patterns the maximum position error is less than $\pm 100 \mu\text{m}$, and there is virtually no separation between the types of event.

B. Centroid shift

We define the ‘ x ’ and ‘ y ’ coordinates as, respectively, parallel to, and orthogonal to, the anode wire direction. An absolute measurement of centroid shift was made by scanning a pencil beam of photons in $200 \mu\text{m}$ steps in the ‘ y ’ direction, across one cell of the detector, i.e. from directly over one field wire to directly over the next field wire, while keeping the ‘ x ’ coordinate fixed. The results for the displaced one & a half chevron are shown in Fig. 8. The scan in Fig. 8(a) was taken over the node

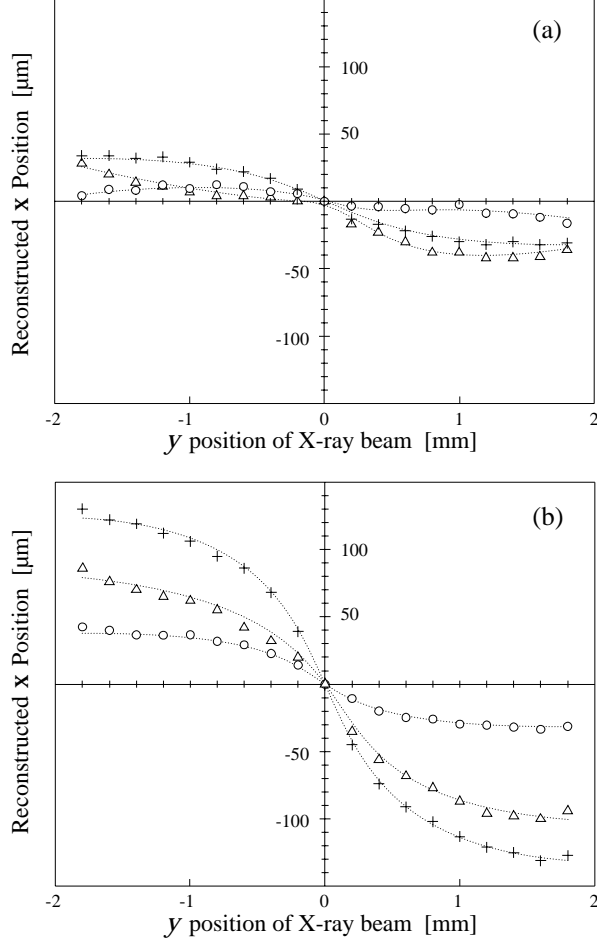


Figure 8: (a) Centroid shift for displaced one & a half chevron, $f_x = 1.05$, over a node. (+ $1.4 \mu\text{sec}$, Δ 500 ns, \circ 100 ns) (b) Same for between nodes

position of the chevron pattern (very close to the chevron apices) and that in Fig. 8(b) was taken midway between nodes. First, it can be seen that centroid shift is worst between nodes, representing movements of about $\pm 120 \mu\text{m}$ at $1.4 \mu\text{sec}$. However, the magnitude decreases as time constant is reduced, because the positive ion cloud from the avalanche has moved a smaller distance away from the side of the anode wire. At 100 nsec, the centroid shift is reduced to about $\pm 30 \mu\text{m}$.

Over a node, centroid shift is of the order $\pm 30 \mu\text{m}$ or less, and is not really a serious problem at any of the time constants. Centroid shift for the displaced single chevron chevron was about a factor five larger than the data shown in Fig. 8. Thus, although the displaced single chevron exhibits differential non-linearity only marginally worse than the one & a half chevron, its significant centroid shift represents a major disadvantage. Centroid shift for the displaced double chevron was very similar to that for the displaced one & a half chevron.

It should be noted that Fig. 8 illustrates centroid shift which is an odd function of ‘ y ’ position of the X-ray beam; this is because the chevron pattern is not a mirror image about the anode wire (when viewed from above — see Fig. 1(d)). Centered chevron patterns, on the other hand, exhibit an even function of centroid shift because the chevron pattern is a mirror image about the anode wire (see Figs.2(a),(c) and (e)).

Theoretical calculations of centroid shift have been carried out, but they require considerably more assumptions to be made about the avalanche process than is the case for DFNL calculations. For example, centroid shift is far more sensitive to parameters such as positive ion mobility and to the degree of angular localization, which determines how broad a fan of positive ions emanates from the anode wire. So far we have not been able to make meaningful comparison between prediction and measurement.

VII. DISCUSSION

This study has been limited to a node spacing, $l_a = 12 \text{mm}$, specifically because we are investigating an alternative position encoding scheme to resistive charge division with the same node spacing, outlined in Ref. [1]. The immediate goal of the study has been to identify a chevron geometry which would yield differential non-linearity of order 10% or less, good position resolution (of order $100 \mu\text{m}$ FWHM), negligible separation in encoded position of pad and window side events, and be largely free of centroid shifts due to avalanche angular localization. It is the latter two effects, in particular, which can result in unexpected non-linearities; in most descriptions of geometric charge division encoders, the effects of angular localization usually receive very little detailed analysis.

We have performed experimental and theoretical evaluations of several chevron patterns which can be fabricated relatively easily, given our dimensional requirements. Some general properties are:

- The displaced versions of the three main chevron types exhibit significantly less differential non-linearity than the centered version (Fig. 3).
- For X-rays, angular localization causes a displacement in recorded position for pad side and window side events. For the centered single chevron, this displacement has a maximum which is larger than the position resolution. In one & a half, and double, chevrons, the effect is small compared with the position resolution, and should not be a concern. We believe that measured displacements of ionizing particle tracks will not be as great as those of X-rays, but we intend to follow this present X-ray study with a similar one using ionizing particles.
- Centroid shift is an odd function of ‘ y ’ position for displaced chevrons, and an even function for centered chevrons. For the single chevron centroid shift is significant at all time constants. For the one & a

half chevron, centroid shift is significant at $1.4\ \mu\text{sec}$ (of order $\pm 100\ \mu\text{m}$), but falls to negligible levels at $100\ \text{nsec}$. Thus it is not a problem for detectors designed for high counting rates.

- d) In fabricating chevron pads on a printed circuit board, it is essential to keep the gap between adjacent pads as small as possible, because an increase in differential non-linearity will otherwise occur.

For our particular experimental requirements, although both versions of the double chevron give excellent performance, the displaced version of the one & a half chevron also exhibits the necessary characteristics, and is a little easier to fabricate.

The results of this investigation should provide valuable guidance in the design of interpolating pad chambers with different dimensions from that used here.

Acknowledgments

We would like to acknowledge the skill and patience of R. Angona and P. Borello in the fabrication of the printed circuit boards containing the chevron pad patterns. We are also grateful for the expert assistance of E. Von Achen and R. Chanda in the fabrication and assembly of the test detector.

B.Y., G.C.S. and V.R. would like to dedicate this paper to the memory of Ernest Mathieson, who passed away on Jan. 1, 1991.

VIII. REFERENCES

1. R. Debbe, J. Fischer, D. Lissauer, T. Ludlam, D. Makowiecki, E. O'Brien, V. Radeka, S. Rescia, L.C. Rogers, G.C. Smith, D. Stephani, B. Yu, S.V. Greene, T.K. Hemmick, J.T. Mitchell and B. Shivakumar, "A study of wire chambers with highly segmented cathode pad readout for high multiplicity charged particle detection," *IEEE Trans. Nucl. Sci.* **NS-37**, 88–94, (1990).
2. A.L.S. Angels, H. Beker, J.C. Berset, G.Di Tore, C.W. Fabjan, U. Goerlach, C. Leroy, M. Price, V. Radeka, B. Sellden, V. Tcherniatine and W.J. Willis, "Test results with a novel high-resolution wire chamber with interpolative pad readout," *Nucl. Instrum. Methods* **A283**, 762–766, (1989).
3. H.O. Anger, "Survey of radioisotope cameras," *Instr. Soc. Am. Trans.* **5**, 311–334 (1966).
4. R. Allemand and G. Thomas, "Nouveau détecteur de localisation," *Nucl. Instrum. Methods* **137**, 141–149, (1976).
5. E. Mathieson, G.C. Smith and P.J. Gilvin, "The graded-density cathode," *Nucl. Instrum. Methods* **174**, 221–225 (1980).
6. C. Martin, P. Jelinsky, M. Lampton, R.F. Malina, and H.O. Anger, "Wedge-and-strip anodes for centroid-finding position-sensitive photon and particle detectors," *Rev. Sci. Instr.* **52**, 1067–1074, (1981).
7. J. Allison, R.J. Barlow, R. Canas, I.P. Duerdoth, F.K. Loebinger, A.A. Macbeth, P.G. Murphy and K. Stephens, "Diamond shaped cathode pads for the longitudinal coordinate from a drift chamber," *Nucl. Instrum. Methods* **A236**, 284–288, (1985).
8. T. Miki, R. Itoh, and T. Kamae, "Zigzag-shaped pads for cathode readout of a time projection chamber," *Nucl. Instrum. Methods* **A236**, 64–68, (1985).
9. E. Mathieson and G.C. Smith, "Reduction in non-linearity in position-sensitive MWPCs," *IEEE Trans. Nucl. Sci.* **NS-36**, 305–310, (1989).
10. V. Radeka and R.A. Boie, "Centroid finding method for position-sensitive detectors," *Nucl. Instrum. Methods* **178**, 543–554, (1980).
11. R.A. Boie, J. Fischer, Y. Inagaki, F.C. Merritt, V. Radeka, L.C. Rogers and D.M. Xi, "High resolution X-ray gas proportional detectors with delay line position sensing for high counting rates," *Nucl. Instrum. Methods* **201**, 93–115, (1982).
12. E. Mathieson and J.S. Gordon, "Cathode charge distribution in multiwire chambers: II. Approximate and empirical formulae," *Nucl. Instrum. Methods* **227**, 277–282, (1984).
13. J. Fischer, V. Radeka and G.C. Smith, "X-ray position detection in the region of $6\ \mu\text{m}$ rms with wire proportional chambers," *Nucl. Instrum. Methods* **A252**, 239–245, (1986).
14. C.J. Borkowski and M.K. Kopp, "Electronic discrimination of the effective thickness of proportional counter," *IEEE Trans. Nucl. Sci.* **NS-24**, 287–292, (1977).